Monthly Notices
of the
ROYAL ASTRONOMICAL SOCIETY

MNRAS **431,** 1005–1018 (2013)
Advance Access publication 2013 March 13

doi:10.1093/mnras/stt153

Search for associations containing young stars: chemical tagging IC 2391 and the Argus association⋆

G. M. De Silva,[1]† V. D'Orazi,[2,3,4] C. Melo,[5] C. A. O. Torres,[6] M. Gieles,[7,8] G. R. Quast[6] and M. Sterzik[5]

[1]*Australian Astronomical Observatory, 105 Delhi Rd, NSW 2113, Australia*
[2]*Macquarie University Astronomy, Astrophysics and Astrophotonics Research Centre, Macquarie University, NSW 2109, Australia*
[3]*Department of Physics and Astronomy, Macquarie University, NSW 2109, Australia*
[4]*Monash Centre for Astrophysics, School of Mathematical Sciences, Building 28, Monash University, VIC 3800, Australia*
[5]*European Southern Observatory, Casilla 19001, Santiago 19, Chile*
[6]*Laboratório Nacional de Astrofísica/MCT, 37504-364, Itajubá, Brazil*
[7]*Institute of Astronomy, University of Cambridge, Madingley Road, Cambridge CB3 0HA, UK*
[8]*Department of Physics, University of Surrey, Guildford, GU2 7XH, UK*

Accepted 2013 January 24. Received 2013 January 23; in original form 2012 October 15

ABSTRACT

We explore the possible connection between the open cluster IC 2391 and the unbound Argus association identified by the search for associations containing young stars survey. In addition to common kinematics and ages between these two systems, here we explore their chemical abundance patterns to confirm if the two substructures shared a common origin. We carry out a homogenous high-resolution elemental abundance study of eight confirmed members of IC 2391 as well as six members of the Argus association using UVES spectra. We derive spectroscopic stellar parameters and abundances for Fe, Na, Mg, Al, Si, Ca, Ti, Cr, Ni and Ba.

All stars in the open cluster and Argus association were found to share similar abundances with the scatter well within the uncertainties, where [Fe/H] $= -0.04 \pm 0.03$ for cluster stars and [Fe/H] $= -0.06 \pm 0.05$ for Argus stars. Effects of overionization/excitation were seen for stars cooler than roughly 5200 K as previously noted in the literature. Also, enhanced Ba abundances of around 0.6 dex were observed in both systems. The common ages, kinematics and chemical abundances strongly support the fact that the Argus association stars originated from the open cluster IC 2391. Simple modelling of this system finds this dissolution to be consistent with two-body interactions.

Key words: stars: abundances – open clusters and associations: general – open clusters and associations: individual: IC 2391 and Argus association.

1 INTRODUCTION

The vast majority of stars that we observe in any given galaxy are field stars, a complex mixture of stellar populations of different ages and metallicities. The present view is that star formation taking place in molecular clouds gives rise to groups of stars – stellar associations and open clusters. These groups of stars must dissolve with time to connect star formation with the field population.

Based on near-infrared studies of embedded clusters, Lada & Lada (2003) suggest that less than about 10 per cent of the clusters formed in molecular clouds survive longer than 10 Myr. They propose that this "infant mortality" of clusters is due to feedback of massive stars that expels the gas from the star-forming region leaving the stars behind with supervirial velocities. For compact systems of a few hundred stars the dynamical time-scale is only a few Myrs. This means that cluster expansion and star loss by two-body relaxation is also a relevant process at these ages for such systems (Gieles, Moeckel & Clarke 2012; Moeckel, Holland & Clarke 2012). On longer time-scales (few 100 Myr)

⋆Based on observations obtained at the European Southern Observatory, Paranal, Chile (ESO program 082.C-0218) and on observations made under the ON-ESO agreement for the joint operation of the 1.52 m ESO telescope and at the Observatório do Pico dos Dias operated by MCT/Laboratório Nacional de Astrofísica (LNA/MCT), Brazil.

† E-mail: gdesilva@aao.gov.au

various processes such as the Galactic tidal field and interactions with giant molecular clouds (GMCs) become important. The paucity of open clusters in the solar neighbourhood with ages between 0.5 and a few Gyr was already noted in the late 1950s (Oort 1958). Spitzer (1958) analytically derived the cluster disruption times due to encounters with GMCs, showing that such phenomena would account for the scarcity of Galactic clusters older than 10^9 yr. A more detailed treatment of the problem taking into account other disruptive agents has been carried out in the literature (e.g. Lamers & Gieles 2006).

Torres et al. (2006) reported the results of a high-resolution optical spectroscopic survey to search for associations containing young stars (SACY) among optical counterparts of *ROSAT* All-Sky X-ray sources in the Southern hemisphere. Using the method described in Torres et al. (2006), Torres et al. (2008) identified nine new young associations, namely Chamaleontis (ChA), TWHydrae (TWA), β Pictoris, Octants (OctA), Tucana-Horologium (THA), Columba (ColA), Carina (CarA), Argus (ArgA) and AB Doradus (ABDA). The age span derived based on the isochrone fitting and the Li abundance analysis ranges from 6 to 70 Myr (da Silva et al. 2009).

Of relevance to the context of cluster disruption discussed above are two young associations identified in the SACY survey which appear to be associated with known open clusters. These are the Argus association and the open cluster IC 2391 and the ϵ Cha Association and the η Cha cluster (Mamajek, Lawson & Feigelson 2000; Torres et al. 2008). In this paper, we investigate in detail the possible connection between the Argus association and the young open cluster IC 2391.

In particular, we can test for a common origin of the association and cluster by examining the stellar elemental abundances. If the abundance analysis reveals high chemical homogeneity among the association stars comparable to the open cluster abundance patterns, it supports a common origin scenario where the Argus association stars were once bound members of open cluster IC 2391. This assumes that the proto-cluster gas cloud was sufficiently mixed hence all stars born from the same site should share the same elemental abundance pattern. This concept of elemental abundance matching is often referred to as *chemical tagging* (Freeman & Bland-Hawthorn 2002). Conversely, if the abundances of the Argus association stars are found to be either heterogeneous, matching the general disc stellar population (e.g. the Hercules stream, see Bensby et al. 2007) or they do not match the abundance patterns of IC 2391, then it is more likely that these are two separate systems even if they share the same kinematics.

Given that disc dynamics make the kinematical information somewhat unreliable to explore the history of these stellar structures, for the first time we carry out a high-resolution elemental abundance analysis of the Argus association in a homogeneous manner with stars in IC 2391 in order to carry out chemical tagging. This will also be the first attempt at chemical tagging a young stellar system. All published examples of chemical tagging in the disc are for stellar systems older than the Hyades (De Silva et al. 2007a; Bubar & King 2010).

In Section 2, we briefly describe the SACY survey and present space velocities and spatial locations of the stars in the two systems. In Section 3, we present a detailed elemental abundance study of stars in both the Argus association and open cluster IC 2391. In Section 4, we discuss our results in terms of chemical tagging the two stellar systems. We conclude with a discussion of possible disruption mechanisms given the evidence gathered in the previous sections.

2 IDENTIFYING THE ARGUS ASSOCIATION IN THE SACY SURVEY

2.1 The convergence method

Usually we think about an association as being a group of stars appearing concentrated in a small volume in space sharing some common properties such as age, chemical composition, distance and kinematics. However, if such a group is close enough to the Sun, its members will appear to cover a large extent in the sky (as an example, Orion at 50 pc would cover almost the whole sky). Thus, to find a group, projected spatial concentrations (i.e. in terms of right ascension and declination only) and proper motions may not be enough. A better criterion is to look for objects sharing similar heliocentric space motions (UVW) all around the sky (where we use U positive towards the Galactic Centre, V positive in the direction of Galactic rotation and W positive in the direction of the North Galactic Pole).

Torres et al. (2006) describe in some detail the convergence method developed to search for members of an association. This method examines the stars in the hexadimensional space, UVWXYZ, as defined by the space motions relative to the Sun and the physical space coordinates centred on the Sun (XYZ, in the same directions as UVW). We represent with m_v, M_v and $M_{v,\mathrm{iso}}$ the apparent visual magnitude, the resultant absolute magnitude with the distance obtained from the convergence method, and the absolute magnitude given by the adopted isochrone for the $(V-I)_C$ stellar colour; and μ_α, μ_δ and V_r are the proper motions and the radial velocity. In brief, if there is no reliable trigonometric distance available,[1] the convergence method finds the distance (d) for each star in the sample that minimizes the F value of equation (1). The first term is a photometric distance modulus and the second is a kinematical one. The method needs, as input, an assumed age and initial velocity values (U_0, V_0, W_0) for the proposed association, and a cutoff value for F above which stars should be considered spurious. This cutoff value varies for each association but usually we begin with 3.5 (this approximately means 0.7 mag for the distance modulus and 3 km s^{-1} for the velocity modulus).

The method is iterative, and for each iteration a list of stars with new (U_0, V_0, W_0) is obtained. The process ends when the list of stars and the velocities (U_0, V_0, W_0) do not change significantly.

$$F(m_v, \mu_\alpha, \mu_\delta, V_r; d) = [p \times (M_v - M_{v,\mathrm{iso}})^2 + (U-U_0)^2 + (V-V_0)^2 + (W-W_0)^2]^{1/2}, \quad (1)$$

where p is a constant weighting the importance of the evolutionary distance with respect to the kinematic distance. Usually, if there are several stars with trigonometric parallaxes among the candidates, we use $p = 0$. But if there are no stars with reliable parallaxes, as is the case for the IC 2391, the method may not converge, so we used $p = 20$ for this case.

We also define a membership probability to verify the compactness of the association in seven dimensions, namely UVWXYZ and $(M_v - M_{v,\mathrm{iso}})$. Normalized values of these variables are computed by subtracting their mean values and dividing by their dispersions.

[1] We consider the trigonometric parallaxes as unreliable if they have errors larger than 2 mas.

A quantity K is obtained as the quadratic sum of these dimensionless variables and the probability is computed as

$$P = 1 - (\mathrm{erf}(k))^7, \quad (2)$$

where erf is the error function.

Finally, we also take into account the Li content of the candidate stars to see if it is compatible with the Li depletion for its age (Neuhäuser 1997).

2.2 Kinematics and ages of IC 2391 and the Argus association

The Argus association was easily discovered in the SACY survey due to its special U velocity of $U = -22.0$ km s^{-1}, as illustrated in fig. 2 of Torres et al. (2008). The pieces of evidence presented in Torres et al. (2008) strongly suggested that the Argus association and IC 2391 have a common origin. We have updated the SACY catalogue in order to be able to test if members proposed by Desidera et al. (2011), Zuckerman et al. (2011) and Riedel et al. (2011) could be converged in to the IC2391 and Argus association member list. Newly obtained data presented in this paper were also used.

The convergence was done using the new reduction of *Hipparcos* (van Leeuwen 2007), the new proper motion catalogue UCAC4 (Zacharias et al. 2012) and the ASAS photometric survey (Kiraga 2012), for V and $V - I$ colours, for stars not observed by us. We did not change the published proper motions for stars in the *Hipparcos* catalogue, and for double stars in UCAC4 with separations between about 1 and 10 arcsec because the image de-blending process in UCAC4 seems unreliable. As we did in Torres et al. (2008), we correct the photometric values for duplicity where possible. Note that for the pair HD 85151A/B, there are no individual proper motions in Tycho-2. Therefore, we used the primary proper motions for both stars. Our spectroscopic observations and the visual binary measurements from the Washington Double Star catalogue suggest they must be a physical pair.

The data for IC 2391 members are mainly from Platais et al. (2007) but using UCAC4 proper motions, except for double stars where we use Platais et al. (2007) and Torres et al. (2008) proper motions due to image de-blending issues with UCAC4 as explained above. There are 41 cluster stars with all kinematical data. Except for PMM 4413 whose systemic velocity is known, all other 20 known spectroscopic binaries were excluded from the study.

In Tables 1 and 2, we list the high-probability members proposed for the Argus association stars and the open cluster IC 2391, respectively, obtained by applying the convergence method for both association and cluster stars together. We present a total of 65 high-probability members which comprise of 32 Argus association stars and 33 IC 2391 members. We accept probabilities down to about 50 per cent as the stellar system is formed by the concentrated IC 2391 cluster and the widely scattered association stars around it, thus forming a spatial distribution that is far from Gaussian. When we apply the convergence criteria on the association stars alone (without including IC 2391 members), then the probabilities of the association members increase significantly with the lowest membership probability being about 70 per cent.)

In order to test the true kinematical connection between IC 2391 and the Argus association stars, we also applied our convergence test to the two groups independently. The results are presented in Table 3 and in Fig. 1. The convergence method resulted in a near perfect match between the kinematics of IC 2391 stars and those of the Argus association stars from Torres et al. (2003). The velocities of the two samples agree well within the errors. To give a better idea of the variations in the final *UVWXYZ* values when the Argus association stars are considered together with the IC 2391 members, we have overplotted the results obtained for the Argus field stars only (red squares), and the IC 2391 members only (blue triangles), with those obtained when the two groups are considered as one single association (grey circles). No significant difference is found.

Also as shown in Table 3 no significant difference is found in the ages of the two groups. Fig. 2 shows that the position of the Argus association in the HR diagram is consistent with a unique isochrone of 30 ± 10 Myr, which is comparable to our obtained age of about 26 Myr. Our ages are from third degree polynomial isochorne curves (Torres et al. 2008) based on some well-observed star groups and compared partially with Siess, Dufour & Forestini (2000). As they are not strictly calibrated, we must take these heuristic ages with caution, but of course the relative ages are more reliable. These results imply that both samples have the same age. Additionally, da Silva et al. (2009) computed Li abundances for all SACY associations and showed that the lithium depletion pattern for the Argus association (defined by fitting the Li abundance as a function of effective temperature), fits well in a time sequence of the SACY associations with no difference between the Argus association stars and the IC 2391 members.

2.3 Comments on excluded stars

Tables 1 and 2 are not the same as those presented in Torres et al. (2008), as we used updated data and applied a new statistical model. Below we comment on the excluded stars.

For the Argus association sample, three stars were excluded from the list of Torres et al. (2008). Star BW Phe was eliminated on kinematical grounds, star CD-49 1902 was eliminated for having too large value in Z and star HD 84075 has a U velocity well outside of the Argus association range.

For the IC 2391 sample, three stars were excluded from the list of Torres et al. (2008). PMM 1560 and PMM 1820 were eliminated due to low membership probabilities based on kinematics. For PMM 3695 the proper motions are significantly distinct between Platais et al. (2007) and UCAC4, for unclear reasons.

3 ELEMENTAL ABUNDANCES

3.1 High-resolution observations

In order to further explore the connection between the open cluster IC 2391 and the Argus association, we examine their elemental abundances. High-resolution and high signal-to-noise (S/N) spectra of members of the Argus association and IC 2391 were observed using VLT-UVES in the framework of programme ID 082.C-0218 (PI Melo). Observations were undertaken in service mode using the UVES DIC#1 (390+580nm) standard setting with a 0.8 arcsec slit to achieve a spectral resolving power of $R = 60\,000$. The typical S/N ratio was ∼100 per pixel at 600 nm. The data were reduced with the latest UVES ESO-MIDAS pipeline. The resulting spectra were normalized using the *continuum* task in the IRAF[2] package.

We carry out a detailed elemental abundance analysis of six Argus association stars and eight IC 2391 stars with $V \sin i \leq 10$ km s^{-1}. The other stars showed broadened spectral lines which meant that there was greater blending between the lines, making individual line

[2] IRAF is distributed by the National Optical Astronomy Observatory, which is operated by the Association of Universities for Research in Astronomy, Inc., under cooperative agreement with the National Science Foundation.

Table 1. Revised list of high-probability members for the Argus association.[1]

Name	α (2000)	δ (2000)	μ_α (mas yr^{-1})	μ_δ	V_r (km s^{-1})	$V \sin i$	$P_{\rm phot}$ (d)	V_J	$V-I_C$	SpT	$E_{\rm Li}$ (mÅ)	$\pi_{\rm kin}$ (mas)	(U, V, W) (km s^{-1})			(X, Y, Z) (pc)			Prob	Notes
(*)CD-29 2360	05 34 59.2	−29 54 04	17.1	33.1	26.0		*3*	*10*	*1*	K3Ve	180	14.8	−22.7	−16.6	−5.2	−34.9	−47.9	−32.4	0.72	K
(*)AP Col	06 04 52.2	−34 33 36	*27*	*340*	*22*	*11*		*12*	*3*	*M4Ve*	*280*	*119.2*	−22.0	−13.6	−4.4	−3.7	−6.7	−3.4	0.90	1
CD-56 1438	06 11 53.0	−56 19 05	−2.5	38.3	14	130	*0*	*11*	*0*	K0V	230	8.7	−21.9	−11.2	−5.1	−9.1	−101.3	−53.3	0.68	K
CD-28 3434	06 49 45.4	−28 59 17	−11.3	20.8	26.8	6.4	*3*	*10*	*0*	G7V	230	9.8	−23.1	−16.3	−7.0	−51.2	−85.3	−23.1	0.45	K
CD-42 2906	07 01 53.4	−42 27 56	−13.8	35.5	23.6	10.8	*3*	*10*	*1*	K1V	275	10.7	−22.8	−16.8	−6.3	−26.5	−85.8	−26.0	0.75	K
CD-48 2972	07 28 22.0	−49 08 38	−26.7	44.4	21.1	52.0	*1*	*9*	*0*	G8V	250	12.6	−22.3	−16.6	−7.3	−11.9	−76.0	−20.0	0.88	K
(*)HD 61005	07 35 47.5	−32 12 14	*−55*	*74*	*22*	*8*	*5*	*8*	*0*	*G8V*	*171*	*28.3*	−23.0	−14.1	−4.4	−14.1	−32.2	−3.5	0.73	H,2
CD-48 3199	07 47 26.0	−49 02 51	−22.4	36.1	18.5	24.7	*2*	*10*	*0*	G7V	230	10.0	−22.2	−15.1	−5.0	−12.9	−96.7	−20.2	1.00	K
CD-43 3604	07 48 49.8	−43 27 06	−26.8	39.6	21.4	40.4	*0*	*11*	*1*	K4Ve	320	12.2	−22.6	−16.4	−4.8	−17.5	−79.1	−12.6	0.82	K
TYC 8561-0970-1	07 53 55.5	−57 10 07	−18.3	26.9	15.8	5.0		*11*		K0V	210	7.0	−21.9	−14.7	−6.5	0.6	−139.0	−36.4	0.98	T
HD 67945	08 09 38.6	−20 13 50	−37.8	20.4	22	120		*8*		F0V	0	14.3	−22.1	−13.4	−4.2	−34.7	−60.0	8.5	0.84	T,SB2?
CD-58 2194	08 39 11.6	−58 34 28	−32.7	35.4	15.6	85.0	*1*	*10*	*0*	G5V	270	9.8	−21.9	−16.7	−5.4	8.3	−100.3	−18.3	0.98	K
CD-57 2315	08 50 08.1	−57 45 59	−34.1	31.0	11.7	52.0		*10*		K2Ve	308	9.3	−22.1	−13.0	−5.5	9.2	−105.8	−16.2	0.90	T
TYC 8594-0058-1	09 02 03.9	−58 08 50	−24.2	26.2	12.1	34.1		11.30	0.83	G8V	300	7.2	−22.2	−14.4	−2.4	15.2	−137.7	−18.7	0.95	
CD-62 1197	09 13 30.3	−62 59 09	−34.1	27.4	12.7	84.0	*0*	10.46	0.93	K0V(e)	280	8.4	−21.7	−16.3	−5.8	22.1	−114.9	−20.4	0.91	K
TYC 7695-0335-1	09 28 54.1	−41 01 19	−28.7	13.6	14	120	*0*	*11*	*1*	K3V	300	6.7	−22.0	−13.6	−5.3	−7.9	−147.3	18.8	0.87	K
(*)BD-20 2977	09 39 51.4	−21 34 17	−50.0	7.8	18.3	10.1		*10*		G9V	260	11.3	−22.3	−16.5	−4.7	−21.9	−79.0	34.4	0.58	T
TYC 9217-0641-1	09 42 47.4	−72 39 50	−30.1	18.9	6.7	23.4	*2*	*12*	*1*	K1V	240	6.5	−22.1	−13.6	−6.2	50.4	−139.6	−39.1	0.88	K
CD-39 5833	09 47 19.9	−40 03 10	−40.6	16.3	15.0	10.5		*10*		K0V	260	9.0	−22.2	−15.7	−4.6	−2.1	−109.5	20.0	0.92	T
HD 85151A	09 48 43.2	−44 54 08	−68.4	33.5	14.3			*9*		G7V	220	15.3	−22.3	−15.8	−3.9	2.5	−64.8	7.7	0.92	T
HD 85151B	09 48 43.4	−44 54 09	−68.4	33.5	13.4			*10*		G9V	250	15.3	−22.3	−14.9	−4.0	2.5	−64.8	7.7	0.84	T
CD-65 817	09 49 09.0	−65 40 21	*−32*	*19*	7.3	19.2	*2*	10.17	0.75	G5V	200	7.1	−22.4	−13.1	−4.8	37.5	−134.5	−22.5	0.97	T,K,D2.0”
HD 309851	09 55 58.3	−67 21 22	−42.4	25.7	6.6	19.8	*1*	9.90	0.68	G1V	170	9.2	−22.5	−13.2	−4.5	31.8	−102.6	−19.0	0.98	K
HD 310316	10 49 56.1	−69 51 22	−43.5	13.5	4.7	16.3	*3*	10.07	0.78	G8V	224	8.2	−22.4	−13.6	−5.2	46.5	−110.7	−19.9	0.97	K,D0.6”
CP-69 1432	10 53 51.5	−70 02 16	−32.6	12.2	3.6	55.0	*1*	10.66	0.71	G2V	195	6.3	−22.8	−13.1	−3.3	61.8	−144.6	−26.1	0.64	K
(*)CD-42 7422	12 06 32.9	−42 47 51	−50.3	−2.5	3.3	28.3	*1*	10.66	0.92	K0V	260	8.9	−21.6	−15.4	−4.8	43.4	−96.5	37.1	0.50	K
CD-74 673	12 20 34.4	−75 39 29	−109.4	4.2	*2*	7.3	*3*	*10*	*1*	K3Ve	230	19.5	−21.7	−15.5	−2.8	25.8	−42.9	−11.5	0.75	K,3,4
CD-75 652	13 49 12.9	−75 49 48	−62.2	−31.5	−0.9	20.1	*2*	9.67	0.76	G1V	200	12.3	−22.3	−13.6	−6.0	47.0	−63.4	−18.8	0.93	K
HD 129496	14 46 21.4	−67 46 16	−47.6	−39.7	−4.8	88.0		8.78	0.60	F7V	150	11.1	−22.5	−13.6	−5.9	61.6	−64.9	−11.5	0.79	
NY Aps	15 12 23.4	−75 15 16	*−73*	*−73*	3.4	10.8	*4*	*9*	*0*	G9V	182	*19.9*	−21.2	−12.6	−4.3	32.3	−36.3	−12.9	0.62	K,H
(*)HD 145689	16 17 05.4	−67 56 29	*−50*	*−84*	*−9*	*106*		*5*	*0*	*A6V*		*19.2*	−22.7	−11.7	−3.7	39.2	−32.4	−11.2	0.68	H,5,6,7
CD-52 9381	20 07 23.8	−51 47 27	85.9	−143.9	−13.3	42.0	*0*	10.59	1.52	K6Ve	60	33.6	−22.4	−14.8	−4.2	24.4	−5.7	−16.0	0.80	K

[1]Data in italics are from the literature as follows: H = data from *Hipparcos*; T = data from TYCHO; K = data from Kiraga (2012); (1) Riedel et al. (2011); (2) Desidera et al. (2011); (3) SB1, $P_{\rm orb}$ = 613.9d Guenther et al. (2007); (4) Covino et al. (1997); (5) Brown dwarf at 6.7 arcsec Huélamo et al. (2010); (6) Zuckerman et al. (2011); (7) Díaz et al. (2011).
Entries marked with asterisks (*) are new inclusions previously not listed by Torres et al. (2008).

Table 2. Revised list of high-probability members proposed for the open cluster IC 2391.[1]

Name	α (2000)	δ (2000)	μ_α	μ_δ	V_r	$V\sin i$	$P_{\rm phot}$	V_J	$B-V$ or $V-I_C$	SpT	$E_{\rm Li}$	$\pi_{\rm kin}$	(U, V, W)			(X, Y, Z)		Prob	Notes
			mas yr^{-1}		(km s^{-1})		(d)				(mÅ)	(mas)	(km s^{-1})			(pc)			
(*)PMM 5314	08 28 34.6	−52 37 04	− 24.1	22.7	13.4	63.0		10.40	0.45			7.1	− 21.7	− 12.2	− 6.3	− 2.5	− 138.5	− 19.6	0.92	
PMM 7422	08 28 45.6	−52 05 27	− 22.6	24.6	14.8	33.0	*1*	10.49	0.69	G6	233	7.2	− 22.1	− 13.7	− 4.8	− 3.5	− 137.1	− 18.6	1.00	K
PMM 7956	08 29 51.9	−51 40 40	− 23.0	18.8	15.3	13.8		10.62	0.98	e	289	6.5	− 21.3	− 13.8	− 7.7	− 4.6	− 152.7	− 19.7	0.71	
PMM 6974	08 34 18.1	−52 15 58	− 22.6	23.0	15.2	5.2	*7*	12.26	1.04		74	6.9	− 22.1	− 14.4	− 5.1	− 2.1	− 143.5	− 18.0	1.00	1
PMM 4280	08 34 20.5	−52 50 05	− 21.0	22.5	12.3	16.0		10.34	0.67	G5	151	6.6	− 22.1	− 11.7	− 4.3	− 0.9	− 151.0	− 19.8	0.90	
PMM 6978	08 35 01.2	−52 14 01	− 23.3	22.3	15.2	7.1	*5*	12.07	1.02		179	6.9	− 22.0	− 14.3	− 5.7	− 2.0	− 143.6	− 17.7	1.00	1
PMM 2456	08 35 43.7	−53 21 20	− 23.6	24.3	14.8	48.0		12.20	0.92	K3e	301	7.2	− 22.1	− 14.3	− 5.0	0.5	− 138.0	− 18.4	1.00	
PMM 351	08 36 24.2	−54 01 06	− 24.4	20.7	15.4	90.0	*1*	10.18	0.57	G0	90	6.8	− 21.6	− 14.8	− 7.3	2.0	− 146.2	− 20.3	0.92	1
PMM 3359	08 36 55.0	−53 08 34	− 23.1	23.6	14.7	8.2	*3*	11.51	0.76		226	7.0	− 22.1	− 14.2	− 4.9	0.3	− 141.6	− 18.2	1.00	1
PMM 5376	08 37 02.3	−52 46 59	− 20.8	20.9	15.6	9.8		14.30	1.37	e	0	6.3	− 22.1	− 15.0	− 5.1	− 0.4	− 158.2	− 19.7	1.00	
PMM 4324	08 37 47.0	−52 52 12	− 22.4	22.0	14.3	41.0		9.66	0.53	F5V	97	6.7	− 22.1	− 13.8	− 5.2	0.0	− 148.9	− 18.5	0.97	
PMM 665	08 37 51.6	−53 45 46	− 21.1	22.7	14.5	7.9	*4*	11.35	0.75	G8e	189	6.5	− 22.2	− 14.3	− 4.4	1.9	− 151.7	− 20.2	1.00	1
PMM 4336	08 37 55.6	−52 57 11	*− 23*	*24*	15.6	8.0	*0*	*11*	*0*	*G9*		7.2	− 22.2	− 15.2	− 4.3	0.1	− 137.9	− 17.2	1.00	1,2
PMM 4362	08 38 22.9	−52 56 48	− 23.5	22.4	15.4	9.0	*3*	*10*	*0*		191	6.9	− 22.0	− 14.7	− 5.6	0.2	− 144.1	− 17.8	1.00	1,2
PMM 4413	08 38 55.7	−52 57 52	− 22.3	21.6	14.4	8.6	*5*	10.31	*0*	*62*	163	6.6	− 22.1	− 13.9	− 5.2	0.4	− 150.9	− 18.5	1.00	1,2,3
PMM 686	08 39 22.6	−53 55 06	− 21.3	21.7	15.2	12.7	*4*	12.63	1.04	e	215	6.4	− 22.1	− 15.1	− 4.9	2.6	− 155.1	− 20.4	1.00	1
PMM 4467	08 39 53.0	−52 57 57	− 21.1	19.3	15.2	12.6	*3*	*11*	*0*	*K0(e)*	*190*	6.1	− 21.9	− 14.7	− 5.9	0.7	− 164.0	− 19.8	1.00	1,2,4
PMM 1083	08 40 06.2	−53 38 07	− 20.0	23.4	12.2	67.9	*1*	*10*	*0*	*G0*	*162*	6.5	− 22.2	− 12.2	− 2.9	2.1	− 152.6	− 19.4	0.92	1,2,4
PMM 8415	08 40 16.3	−53 56 29	− 25.7	24.9	15.7	20.7		*11*	*0*	*G9(e)*	*302*	7.6	− 22.1	− 15.3	− 5.2	0.6	− 131.2	− 15.7	1.00	2,4
PMM 1759	08 40 18.3	−53 30 29	− 26.2	21.2	13.5	3.8		*13*	*1*	*K4e*	*55*	7.1	− 21.6	− 13.0	− 7.0	1.8	− 139.1	− 17.4	0.94	2,4
PMM 1142	08 40 49.1	−53 37 45	− 18.4	23.6	14.0	7.3		*11*	*0*	*G1*		6.3	− 22.1	− 14.2	− 2.0	2.4	− 156.4	− 19.6	0.91	2
PMM 1174	08 41 22.7	−53 38 09	− 23.6	22.7	13.5	60.0		9.54	0.43	F3V	79	6.9	− 22.1	− 13.3	− 5.1	2.3	− 144.2	− 18.0	1.00	
PMM 4636	08 41 57.8	−52 52 14	− 24.0	23.9	13.6	4.9	*5*	*13*	*1*	*K7e*	*100*	7.2	− 22.2	− 13.3	− 4.5	0.9	− 138.8	− 16.0	1.00	1,2,4
PMM 756	08 43 00.4	−53 54 08	− 23.5	20.4	15.9	16.5	*3*	11.16	0.68	G9	217	6.5	− 21.8	− 15.7	− 6.4	3.4	− 152.1	− 18.9	0.98	1
PMM 5811	08 43 17.9	−52 36 11	− 21.3	21.6	14.3	59.0		9.16	0.37	F2V	107	6.4	− 22.2	− 14.0	− 4.2	0.7	− 155.0	− 17.0	0.97	
PMM 2888	08 43 52.3	−53 14 00	− 25.3	20.2	15.0	66.5		*9*	*0*	*F5*		6.9	− 21.6	− 14.6	− 7.0	2.1	− 144.7	− 16.6	0.96	2
PPM 2012	08 43 59.0	−53 33 44	*− 24*	*25*	13.9	17.4	*2*	*11*	*0*	*K0(e)*	*251*	7.4	− 22.2	− 13.9	− 4.3	2.6	− 134.5	− 15.9	1.00	1,2,4
PMM 4809	08 44 05.2	−52 53 17	− 21.3	19.7	13.8	17.5	*2*	*10*	*0*	*G3(e)*	175	6.1	− 22.1	− 13.5	− 5.2	1.6	− 162.6	− 18.0	1.00	1,2
PMM 1373	08 44 10.2	−53 43 34	*− 23*	*24*	14.6	7.0	*5*	12.25	0.96		156	7.1	− 22.2	− 14.7	− 4.0	3.1	− 140.5	− 16.8	1.00	1
PMM 5884	08 44 26.2	−52 42 32	− 21.4	17.5	14.5	13.9	*3*	*11*	*0*	*G9(e)*	*225*	5.8	− 21.8	− 14.1	− 6.5	1.4	− 170.2	− 18.4	0.98	1,2,4
PMM 4902	08 45 26.9	−52 52 02	− 25.2	23.4	14.7	7.7	*4*	*12*	*1*	*K3e*	*204*	7.2	− 22.1	− 14.5	− 5.1	1.6	− 137.5	− 14.8	1.00	1,2,4
PMM 6811	08 45 39.1	−52 26 00	*− 24*	*24*	17.4	90.0	*0*	*9*	*0*	*F8)*	137	7.3	− 22.2	− 17.2	− 4.2	0.9	− 135.4	− 13.9	0.96	2
PMM 2182	08 45 48.0	−53 25 51	*− 22*	*22*	14.7	78.0	*1*	10.22	0.57		187	6.6	− 22.2	− 14.7	− 4.4	3.1	− 150.4	− 17.0	1.00	1

[1]Data mainly from Platais et al. (2007); those in italics are from other literature sources as indicated (for proper motions, data in italics are from Platais et al. (2007), otherwise from UCAC4; for colour indices, data in italics represent $V-I_C$.): K = data from Kiraga (2012); (1) Desidera et al. (2011); (2) Patten & Simon (1996); (3) SB2, $P_{\rm orb} = 90.617$ d Platais et al. (2007) (4) Randich et al. (2001).
The entry marked with an asterisk (*) is a new inclusion previously not listed by Torres et al. (2008).

Table 3. Convergence method results for the Argus field stars and the members of open cluster IC 2391.

Sample	Distance (mas)	U (km s^{-1})	V (km s^{-1})	W (km s^{-1})	N. members	Age (Myr)
Argus only (field)	15.5 ± 19.9	-22.6 ± 0.4	-14.6 ± 1.5	-5.0 ± 1.2	32	26
IC 2391	6.9 ± 0.4	-21.7 ± 0.6	-14.2 ± 1.0	-5.1 ± 1.2	33	26
Argus and IC 2391	11.2 ± 14.5	-22.1 ± 0.4	-14.4 ± 1.3	-5.0 ± 1.2	65	26

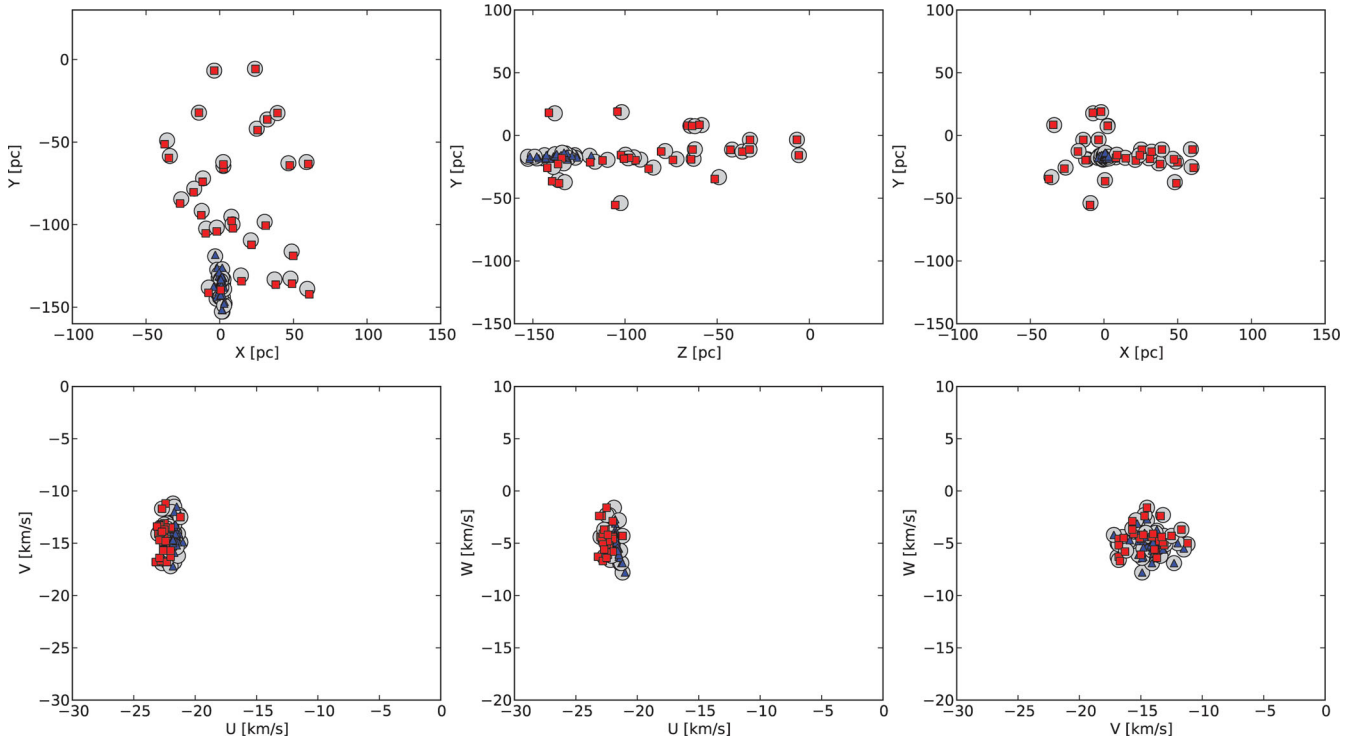

Figure 1. Combinations of the UVWXYZ–space derived based on the convergence method for the Argus association stars (red squares), the open cluster IC 2391 (blue triangles) and when the two systems are considered as a single association (grey circles). Well-defined clustering can be seen in both kinematical and spatial coordinates, with no significant difference when considering the two stellar system independently or together.

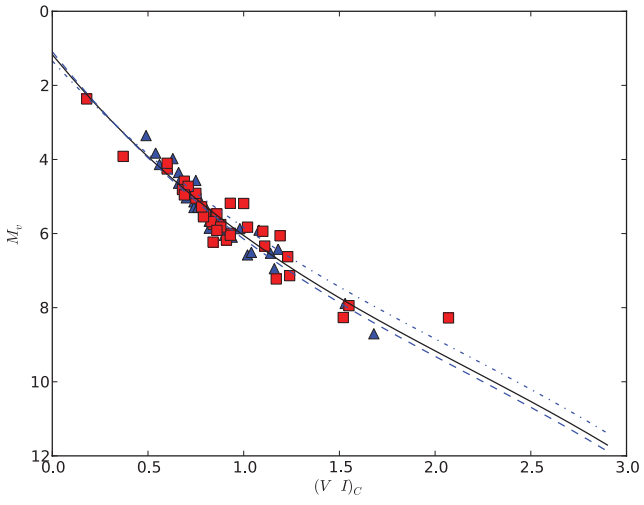

Figure 2. The HR diagram of the members proposed for the Argus association. The blue triangles are the ArgA field members, whereas the IC 2391 members are represented by the red triangles. The overplotted isochrones (Siess et al. 2000) are the ones for 20 (dot–dashed), 30 (solid) and 40 Myr (dashed).

analysis more uncertain. Table 4 lists the sample of stars analysed in this study together with their measured properties.

3.2 Abundance analysis

The elemental abundances were derived based on equivalent width (EW) measurements and spectral synthesis, making use of the latest version of the MOOG code (Sneden 1973). The EWs were measured using the automated ARES code (Sousa et al. 2007) with frequent manual checking of the EWs. Ba abundances were derived from the 5853 Å line (which is known to be strong, isolated, un-blended and not affected by Non-Local Thermodynamic Equilibrium (NLTE) effects, e.g. Mashonkina et al. 2007) using the driver *synth* in MOOG. We retrieved hyperfine structure data from McWilliam et al. (1995), adopting an isotopic solar mixture of 81 per cent (^{134}Ba +^{136}Ba +^{138}Ba) and 19 per cent (^{135}Ba +^{137}Ba). An example of the synthesis of the Ba II line at 5853 Å is provided in Fig. 3 for one of our sample stars (PMM 3359).

Interpolated Kurucz model atmospheres based on the ATLAS9 code (Castelli, Gratton & Kurucz 1997) with no convective overshooting were used throughout this study. We carried out the abundance analysis relative to the solar spectrum, taken with the same instrument and the same resolution of our sample stars. The full lines list, atomic data adopted and measured EWs of a sample star (PMM 3359) can be found in Appendix A.

Table 4. Stellar parameters and abundances (see Section 3.4 for details on the computation of the average values).

star	RV (km s^{-1})	$V\sin i$ (km s^{-1})	$T_{\rm eff}$ (K)	logg	ξ (kms^{-1})	[Fe I/H]	[Fe II/H]	[Na/Fe]	[Mg/Fe]	[Al/Fe]	[Si/Fe]	[Ca/Fe]	[Ti I/Fe]	[Ti II/Fe]	[Cr I/Fe]	[Cr II/Fe]	[Ni/Fe]	[Ba II/Fe]
IC 2391																		
PMM 4902	14.7	7.10	4440	4.5	1.3	-0.03 ± 0.12	–	-0.25 ± 0.15	-0.06 ± 0.09	-0.08 ± 0.06	0.09 ± 0.08	-0.25 ± 0.11	-0.32 ± 0.17	0.12 ± 0.14	-0.07 ± 0.15	0.41 ± 0.23	0.03 ± 0.09	0.65 ± 0.15
PMM 6974	15.1	4.99	4600	4.5	1.2	-0.06 ± 0.08	–	-0.21 ± 0.14	-0.06 ± 0.09	-0.09 ± 0.04	0.17 ± 0.09	-0.29 ± 0.10	-0.33 ± 0.09	0.14 ± 0.15	-0.14 ± 0.13	0.32 ± 0.14	0.03 ± 0.10	0.60 ± 0.15
PMM 6978	15.4	6.77	4600	4.5	1.1	-0.01 ± 0.10	–	-0.26 ± 0.13	-0.07 ± 0.05	-0.12 ± 0.09	0.12 ± 0.10	-0.29 ± 0.11	-0.31 ± 0.13	0.11 ± 0.13	-0.10 ± 0.09	0.22 ± 0.18	0.03 ± 0.09	0.65 ± 0.15
PMM 1373	13.9	6.68	4750	4.5	1.2	-0.05 ± 0.10	–	-0.16 ± 0.12	-0.11 ± 0.09	–	0.10 ± 0.09	-0.19 ± 0.09	-0.27 ± 0.15	0.15 ± 0.15	-0.03 ± 0.07	0.44 ± 0.22	0.02 ± 0.10	0.65 ± 0.15
PMM 3359	14.7	7.88	5380	4.5	1.2	0.00 ± 0.10	–	0.02 ± 0.08	0.01 ± 0.07	-0.01 ± 0.07	-0.05 ± 0.08	0.08 ± 0.10	-0.03 ± 0.12	0.04 ± 0.11	0.00 ± 0.09	0.09 ± 0.12	-0.03 ± 0.11	0.65 ± 0.15
PMM 665	14.6	7.47	5550	4.5	1.6	-0.07 ± 0.08	-0.11 ± 0.12	0.05 ± 0.08	0.05 ± 0.09	0.09 ± 0.04	0.07 ± 0.07	0.08 ± 0.09	0.07 ± 0.09	0.04 ± 0.14	0.03 ± 0.09	0.08 ± 0.09	0.03 ± 0.09	0.46 ± 0.15
PMM 4362	15.1	8.61	5650	4.3	1.4	-0.05 ± 0.10	-0.08 ± 0.09	0.09 ± 0.07	0.03 ± 0.08	0.08 ± 0.04	0.05 ± 0.07	0.11 ± 0.09	0.01 ± 0.11	0.03 ± 0.11	0.11 ± 0.11	0.10 ± 0.07	0.02 ± 0.11	0.60 ± 0.20
PMM 1142	14.0	6.71	5700	4.3	1.5	-0.07 ± 0.09	-0.05 ± 0.11	0.10 ± 0.09	0.03 ± 0.09	0.06 ± 0.04	0.02 ± 0.06	0.08 ± 0.09	0.09 ± 0.11	-0.02 ± 0.11	0.06 ± 0.06	0.02 ± 0.06	-0.01 ± 0.10	0.70 ± 0.15
AVERAGE ± rms					-0.04 ± 0.03	-0.08 ± 0.03	0.06 ± 0.04	0.03 ± 0.02	0.06 ± 0.05	0.02 ± 0.05	0.09 ± 0.02	0.04 ± 0.06	0.02 ± 0.03	0.05 ± 0.05	0.07 ± 0.04	0.02 ± 0.03	0.62 ± 0.07	
ARGUS																		
CD-74 673	4.8	7.28	4600	4.5	1.3	0.04 ± 0.10	–	-0.22 ± 0.13	-0.11 ± 0.06	-0.01 ± 0.11	0.10 ± 0.10	-0.22 ± 0.12	-0.19 ± 0.15	0.03 ± 0.13	-0.11 ± 0.13	0.19 ± 0.13	0.01 ± 0.11	0.55 ± 0.15
TYC 8561-0907-1	15.6	4.41	4900	4.5	1.2	-0.10 ± 0.09	–	-0.20 ± 0.13	-0.11 ± 0.06	-0.09 ± 0.08	0.17 ± 0.09	-0.14 ± 0.11	-0.37 ± 0.13	0.21 ± 0.11	-0.19 ± 0.11	0.44 ± 0.15	0.01 ± 0.09	0.65 ± 0.15
CD-42 2906	23.5	10.35	5200	4.5	1.6	-0.07 ± 0.09	–	0.01 ± 0.08	0.04 ± 0.08	0.02 ± 0.05	0.08 ± 0.09	0.04 ± 0.11	-0.02 ± 0.09	0.01 ± 0.14	0.03 ± 0.09	0.12 ± 0.09	0.02 ± 0.06	0.45 ± 0.20
NY Aps	−3.2	10.95	5340	4.5	1.5	-0.03 ± 0.10	–	0.09 ± 0.11	0.08 ± 0.09	0.04 ± 0.06	0.05 ± 0.09	0.14 ± 0.11	0.07 ± 0.10	0.02 ± 0.11	0.07 ± 0.10	0.17 ± 0.19	-0.03 ± 0.07	0.45 ± 0.15
CD-39 5833	14.9	10.17	5500	4.6	1.6	-0.02 ± 0.10	-0.04 ± 0.09	0.01 ± 0.06	-0.02 ± 0.08	0.00 ± 0.05	-0.05 ± 0.09	0.09 ± 0.09	0.06 ± 0.10	0.05 ± 0.13	0.11 ± 0.06	0.15 ± 0.11	0.00 ± 0.07	0.60 ± 0.20
CD-28 3434	26.8	6.36	5600	4.3	1.5	-0.09 ± 0.09	-0.10 ± 0.08	0.07 ± 0.07	0.02 ± 0.08	0.05 ± 0.07	0.01 ± 0.09	0.13 ± 0.09	0.00 ± 0.11	-0.07 ± 0.15	0.11 ± 0.09	0.13 ± 0.15	0.00 ± 0.06	0.50 ± 0.15
AVERAGE ± rms						-0.05 ± 0.05	-0.07 ± 0.04	0.05 ± 0.04	0.03 ± 0.04	0.03 ± 0.02	0.02 ± 0.06	0.09 ± 0.05	0.03 ± 0.04	0.00 ± 0.05	0.08 ± 0.04	0.14 ± 0.02	0.00 ± 0.02	0.53 ± 0.08

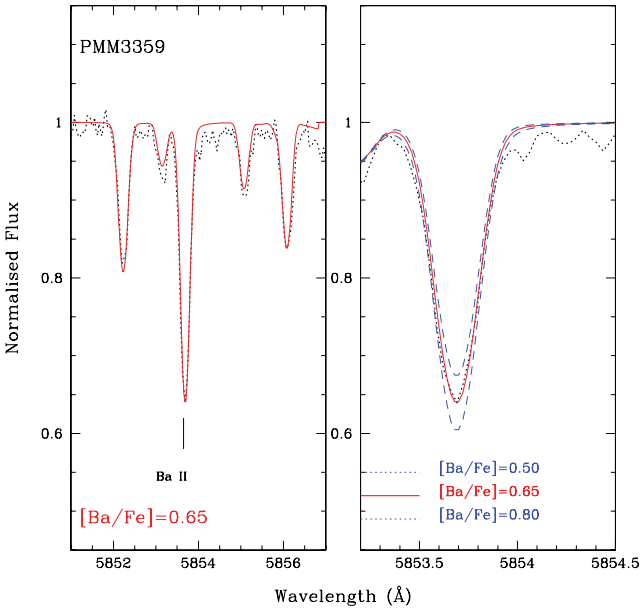

Figure 3. Example of the Ba synthesis for star PMM 3359, with solid red line showing the best fit.

We derive the stellar parameters based on spectroscopy. Abundances for all Fe I and II lines were computed from the measured EWs. Effective temperature ($T_{\rm eff}$) was derived by requiring excitation equilibrium of the Fe I lines. Microturbulence was derived from the condition that abundances from Fe I lines show no trend with EW. Surface gravity (log g) was derived via ionization equilibrium, i.e. requiring the abundances from Fe I lines to equal those from Fe II lines. For stars cooler than 5500 K, we adopted a log g value of 4.5, which is consistent with the cluster age. We did not attempt to optimize log g via ionization equilibrium for the cool stars because of the known overionization effects (e.g. Schuler et al. 2010, see Section 3.4 for further discussion). The final adopted stellar parameters and the elemental abundances are given in Table 4.

3.3 Error budget

Chemical abundances are mainly affected by two kinds of uncertainties, namely (*i*) errors due to the EW measurements or to the best-fitting determination (in the case of spectral syntheses), and (*ii*) errors due to the stellar parameters ($T_{\rm eff}$, log g and ξ). The impact of the uncertainties on the atomic parameters, i.e. log gf, should be instead almost negligible since our analysis is strictly differential with respect to the Sun (see Section 3.2). Concerning the EW analysis, random errors in the [Fe/H] ratios due to EW measurements are well represented by the standard deviation (rms) from the mean abundance based on the whole set of lines, while the ones for the [X/Fe] ratios were computed by quadratically adding the root mean square (rms) for [Fe/H] and rms for [X/H]. Errors due to stellar parameters were estimated by varying one parameter at a time, and checking the corresponding variation in the resulting abundance. We adopted variations of $\pm$50 K in $T_{\rm eff}$ and $\pm$0.15 km s^{-1} in ξ, because larger changes in those quantities would have introduced a significant trend of log n(Fe) versus the excitation potentials and the line strength, respectively. For stars for which we could optimize the surface gravities, the uncertainties in log g were estimated by varying this quantity until the difference between log n(Fe I) and log n(Fe II) is larger than 0.1 dex, i.e. the ionization equilibrium condition is no longer satisfied. The typical error in log g was from 0.1 to 0.15. The final errors are then obtained by quadratically summing errors due to the EW measurements and the ones due to stellar parameters (see Table 4).

Focusing on abundances derived from spectral syntheses, we have errors due to the best-fitting determination of typically 0.1 dex, reflecting uncertainties due to the continuum placement and to the strong nature of the Ba features; similarly, since we are dealing with a very strong transition line, the errors due to stellar parameters are dominated by the microturbulence values (Δ[Ba/Fe] = 0.05–0.07 dex for ξ changes of 0.15 km s^{-1}), while the effective temperatures and gravities have a minor impact, i.e. within 0.03 dex.

3.4 Abundance results

Final abundances are reported in Table 4, where stellar parameters ($T_{\rm eff}$, log$g$, ξ) and [X/Fe] ratios along with the corresponding errors are provided for all our sample stars. In Fig. 4, we show the [X/Fe] ratios as a function of the effective temperatures for both IC 2391 (filled circles) and the Argus association (triangles). The first evidence coming out from these plots is that we confirm previous findings by Schuler et al. (2003), Schuler et al. (2004), Shen et al. (2005), D'Orazi & Randich (2009), Schuler et al. (2010) and Biazzo et al. (2011): overionization/excitation effects are at work for stars cooler than $T_{\rm eff} \lesssim 5200$ K. The photospheric abundances of Ca, Na and Ti (from the Ti I lines) show the most dramatic effect of this phenomenon, being about 0.2–0.3 dex lower in the cooler stars; similarly, Al and Cr (from the Cr I lines) seem to show the same effect, although to a lesser extent. Because we could also measure abundances for Cr and Ti from their first-ionization stage transitions, we can confirm that we are observing an overionization phenomenon: as can be seen in Table 4, abundances from Ti II and Cr II lines result in larger values for the cooler stars, where the [X/Fe] ratios are enhanced up to 0.4 dex (see the [Cr II/Fe] in the most extreme cases, e.g. PMM 4902 in IC 2391 or TYC 8561-0907-1 in Argus association). This fact reflects a pumping of the electrons to the ionized stage because of the strong UV flux coming from the hot chromospheres [we refer the reader to Schuler et al. (2003, 2010); D'Orazi & Randich (2009) for a more detailed discussion on this topic]. Si deserves special attention since we found an overexcitation effect (all the employed lines have high excitation potentials, i.e. $4.92 < \chi < 5.98$ eV) acting on the cooler stars, which was also previously detected by Schuler et al. (2003) in M34, but not by D'Orazi & Randich (2009). Overionization/excitation effects are also observed in the cool field stars (see e.g. Allende Prieto et al. 2008). Note that no temperature effects were observed for the Ni abundances in either the IC 2391 or the Argus association stars. Therefore, the Ni abundance is not plotted in Fig. 4.

Due to the overionization effects, the mean abundances and the associated rms error were computed considering all the stars for Fe I, Mg, Ni and Ba, while we considered only the warmer stars ($T_{\rm eff} >$ 5200 K) when averaging [X/Fe] ratios for Na, Al, Si, Ca, Ti and Cr (see Table 4). We found average metallicity of [Fe/H] = -0.04 ± 0.03 and [Fe/H] = -0.05 ± 0.04 for IC 2391 and Argus association, respectively: the cluster and the association exhibit a solar metallicity, with no evidence of internal scatter (the rms is significantly smaller than the observational uncertainties). Moreover, all the other α (Mg, Si, Ca and Ti), odd-Z (Na, Al), and iron-peak elements show solar ratios, pointing out that the cluster and the association are indistinguishable concerning their chemical composition (see Section 4 for a discussion on the scientific implication of our results).

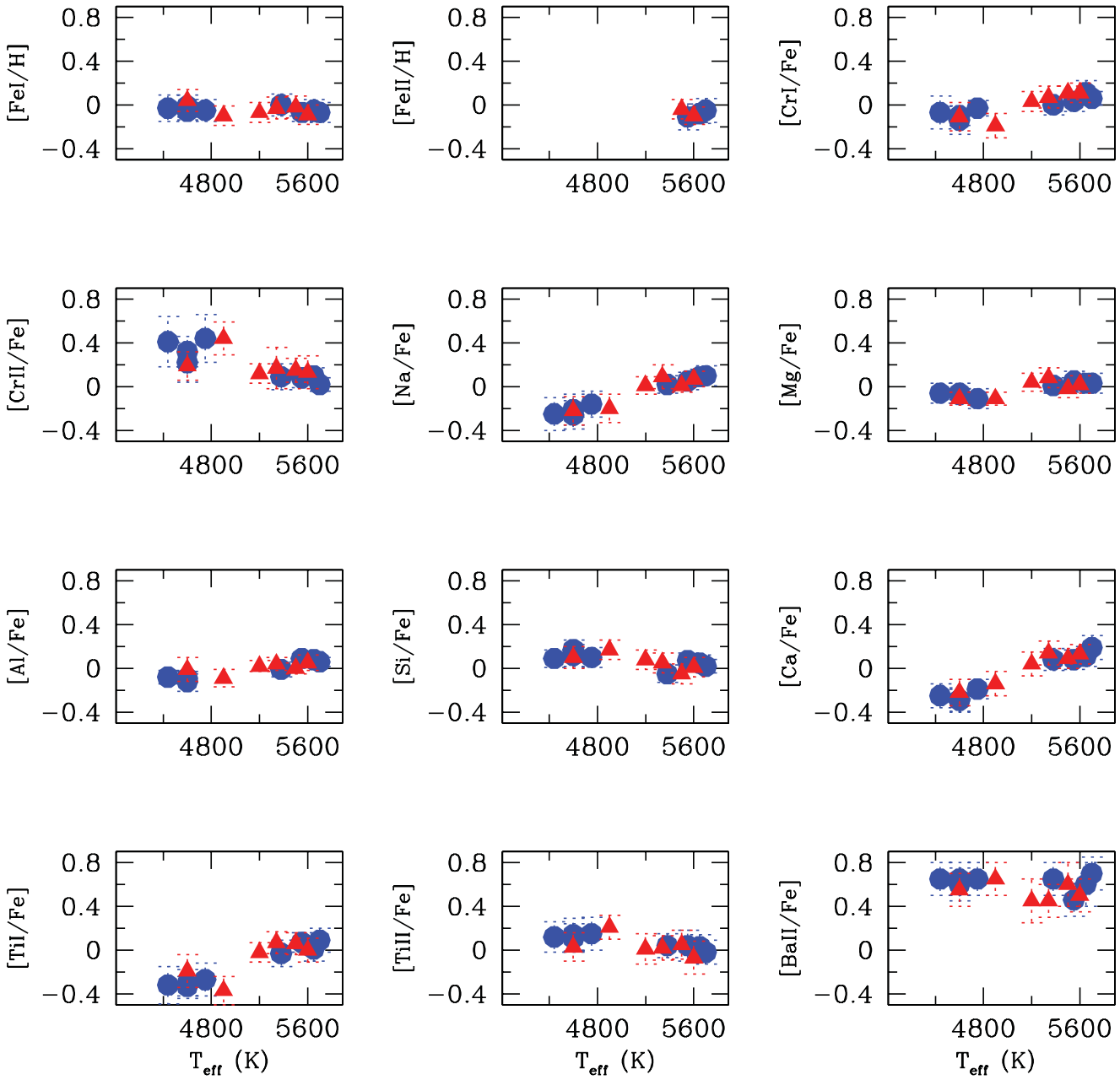

Figure 4. [X/Fe] ratios as a function of the effective temperatures, showing the effects of overionization. Note that [Ni/Fe] is not included as the Ni abundances do not show any temperature-dependent trends (see Table 4). The circles show IC 2391 stars and the triangles show Argus association stars.

Ba is notably overabundant, with a mean of [Ba/Fe] = 0.62 ± 0.07 (IC 2391) and [Ba/Fe] = 0.53 ± 0.08 (Argus association). The slightly higher variation across the two stellar aggregates mainly reflects the larger uncertainties affecting Ba abundances. The Ba line feature is close to the saturation regime in the curve of growth, and as a consequence it is highly sensitive to the adopted microturbulence values. The extremely high Ba content that we obtained for our sample stars is not surprising and confirms previous measurements (see Section 4). We stress, in passing, that overionization effects can be ruled out as a possible explanation given that, at the effective temperatures of our sample stars, Ba is almost totally ionized. Further, the possibility of NLTE effects is minimal as the 5853 line used in this study is not known to be affected by NLTE effects (Mashonkina et al. 2007).

3.5 Comparison with previous abundance studies

The chemical composition of IC 2391 has been previously determined by two different studies, namely Platais et al. (2007, hereafter P07) and D'Orazi & Randich (2009).

In P07, the authors presented iron abundances for a sample of four G-type members, obtaining an average metallicity of [Fe/H] = 0.05 ± 0.05, which is in very good agreement with our estimate. Three out of four P07 stars are in common with our study, i.e. PMM 3359, PMM 665 and PMM 4362; the differences in effective temperatures are $\Delta T_{\rm eff}$(our−p07) = 100, 99 and 34 K, respectively, while gravities agree within 0.05 dex. Microturbulence values agree very well for the star PMM 3359 ($\Delta\xi$ = 0.03 km s^{-1}) and PMM 4362 ($\Delta\xi$ = 0.1 km s^{-1}), while P07 derived a slightly lower value

Table 5. Comparison between our study and the one by D'Orazi & Randich (2009) for two stars in common.

star	$T_{\rm eff}$ (K)	logg	ξ (km s^{-1})	[Fe/H]	[Na/Fe]	[Si/Fe]	[Ca/Fe]	[TiI/Fe]	[TiII/Fe]	[Ni/Fe]
PMM 4362	5650 ± 50	4.30 ± 0.10	1.40 ± 0.15	-0.05 ± 0.10	0.09 ± 0.07	0.05 ± 0.07	0.11 ± 0.09	0.01 ± 0.11	0.03 ± 0.11	0.02 ± 0.11
PMM $4362_{\rm DR09}$	5590 ± 60	4.45 ± 0.10	1.15 ± 0.15	0.00 ± 0.08	-0.02 ± 0.07	0.02 ± 0.07	0.01 ± 0.05	0.00 ± 0.07	0.03 ± 0.10	-0.02 ± 0.07
PMM 4902	4440 ± 50	4.50 ± 0.15	1.30 ± 0.15	-0.03 ± 0.12	-0.25 ± 0.15	0.09 ± 0.08	-0.25 ± 0.11	-0.32 ± 0.17	0.12 ± 0.14	0.03 ± 0.09
PMM $4902_{\rm DR09}$	4343 ± 60	4.50 ± 0.10	1.20 ± 0.15	0.00 ± 0.09	-0.34 ± 0.11	0.06 ± 0.12	-0.38 ± 0.14	-0.35 ± 0.17	0.37 ± 0.14	0.02 ± 0.12

for the star PMM 665, i.e. 1.25 km s^{-1} to be compared with our estimate of 1.60 km s^{-1}.

D'Orazi & Randich (2009) presented abundances of Na, α − (Si, Ca and Ti), and iron-peak elements (Fe and Ni) for a sample of seven IC 2391 G-/K-type members. They found the following average values: [Fe/H] = -0.01 ± 0.02, [Na/Fe] = -0.02 ± 0.03, [Si/Fe] = 0.01 ± 0.02, [Ca/Fe] = 0.02 ± 0.01, [Ti I/Fe] = 0.00 ± 0.02, [Ti II/Fe] = 0.14 ± 0.13 and [Ni/Fe] = 0.00 ± 0.02. Comparing their results with our mean abundances (see Table 4), we can conclude that the two studies are in excellent agreement; the only exception is the Ti abundances derived from the Ti II lines, for which they obtained a 0.12 dex higher value. Note that their [Ti II/Fe] average was based on all sample stars, including those with overionization effects. Should we include all sample stars when determining the average, then our abundance estimates would agree well. Two of our sample stars, PMM 4902 (VXR 76a) and PMM 4362 (VXR 3), were already analysed by D'Orazi & Randich (2009). In Table 5, we compare our results with the ones by D'Orazi & Randich (2009): the two determinations agree within their respective uncertainties for all stellar parameters and final abundances. We note that the higher discrepancy for the Ti abundance from the Ti II lines is still within the uncertainties, which are significantly larger in this case (a different set of line list could partially explain such a difference). The barium abundance for IC 2391 is presented in D'Orazi et al. (2009), where they derived a mean abundance of [Ba/Fe] = 0.68 ± 0.07, which is in excellent agreement with our value ([Ba/Fe] = 0.62 ± 0.07).

The chemical content of the Argus association was previously determined by Viana Almeida et al. (2009), who gathered Fe, Si and Ni abundances for a sample of seven members. They also conclude that the association shows a solar abundance pattern, finding [Fe/H] = -0.03 ± 0.05,[3] [Si/Fe] = -0.03 ± 0.03 and [Ni/Fe] = 0.02 ± 0.04. We have four stars in common with the work by Viana Almeida et al. (2009), namely CD-28 3434, CD-42 2906, TYC 8561-0970-1 and CD-38 583. Differences in $T_{\rm eff}$ are within 100K for all the stars with the exception of TYC 8561-0970-1 for which we derived a $T_{\rm eff}$ = 4900 K, while their final estimate is $T_{\rm eff}$ = 5348 K. However, our final value agrees better with the spectral type K0 found by Torres et al. (2006) (see Table 1) compared to that by Viana Almeida et al. (2009). Moreover, while gravity values agree well (with an average difference of 0.125), larger discrepancies are seen for the microturbulence values. Viana Almeida et al. (2009) derived systematically higher microturbulences (on average about 0.15 km s^{-1} higher, which is still in fair agreement within the uncertainties) and noted that their higher ξ values are probably due to a different set of spectral lines, which might be particularly sensitive to the strong magnetic field characterizing these stars, resulting in larger ξ values. Whether young pre-main-sequence stars exhibit higher microturbulence values is still under discussion and there is no general consensus on this topic (Steenbock & Holweger 1981; James et al. 2006). Finally, [Fe/H], [Si/Fe] and [Ni/Fe] agree well among the two studies, with differences always smaller than 0.1 dex.

[3] We quote their uncorrected value, and refer the reader to that paper for details on the trends with effective temperatures among their sample stars.

4 DISCUSSION

4.1 Chemical tagging

Stars born within a single star-forming aggregate share their chemical signature with all stars in the cluster, where the elemental abundance pattern represents the conditions of the proto-cluster gas cloud. High-resolution studies targeting a large range of chemical elements have confirmed this to be true among several Galactic open clusters (e.g De Silva et al. 2006, 2007b; Pancino et al. 2010). Indeed, the results presented in Table 4 show that the open cluster IC 2391 is also highly chemically homogeneous, with any abundance scatter being well within the measurement uncertainty.

The technique of chemical tagging proposes to use the elemental abundance patterns of stars to identify dispersed field stars with their original formation site (Freeman & Bland-Hawthorn 2002). Several recent examples show the concept of chemical tagging at work: the HR 1614 moving group (De Silva et al. 2007a), the Hercules stream (Bensby et al. 2007), the Wolf 630 moving group (Bubar & King 2010) and the Hyades Supercluster (De Silva et al. 2011; Pompéia et al. 2011). In all these examples the dispersed stellar system was identified via kinematical information and its reality as a disrupting cluster was confirmed (or disproved in the case of the Hercules stream) via chemical abundances. Similarly, the presence of the Argus association was identified by the stellar kinematics in the SACY survey and has been kinematically associated with the open cluster IC 2391, see Fig. 1. Probing the chemical information of their stars, we show in Table 4, the average elemental abundances between the open cluster stars and the dispersed members of the Argus association are almost identical within the uncertainties. This similarity holds for all studied elements, which include those formed via the α-process, Fe-peak elements formed via nuclear fusion and *s*-process elements formed via neutron capture. This seems to support the case that the stars in the Argus association originally formed together with the open cluster IC 2391. Note that unlike the previous cases of chemically tagged stellar structures, IC 2391 and the Argus association are young stellar systems, with an age of ∼30 Myr as presented in Table 3.

We now compare the cluster and association abundances against the solar neighbourhood abundances published by Bensby et al. (2005). As seen in Fig. 5, most of the abundances of the studied structures sit well within the solar neighbourhood values. Therefore, this lessens the strength of the chemical tagging argument discussed above, as other field stars may also share a similar chemical abundance pattern as that of the IC 2391. Applying the method

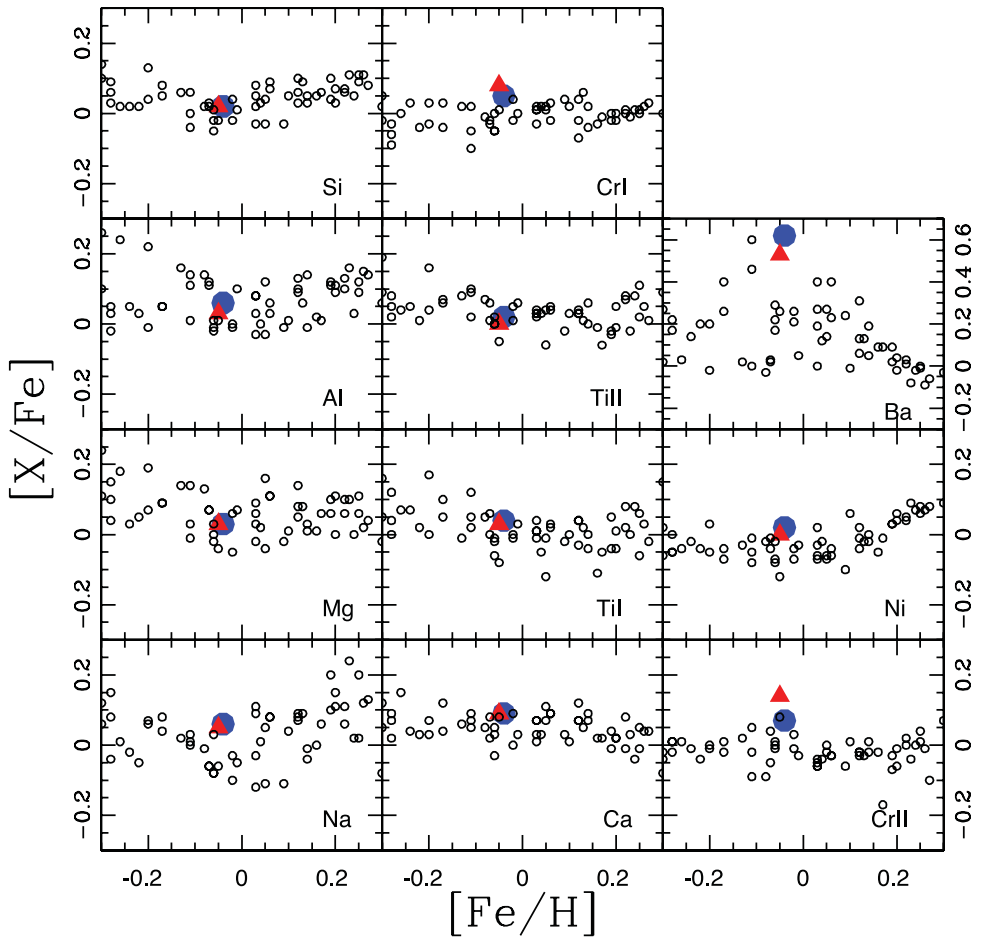

Figure 5. The average abundances for IC 2391 cluster (blue circle) and Argus association stars (red triangle) compared to the solar neighbourhood abundances of Bensby et al. (2005) (open circles). The average abundance values plotted here do not include the stars which show effects of overionization. Refer to section 3.4 for details on how the average abundances were derived.

of chemical tagging, we consider the number of stars in the Bensby et al. (2005) sample which share the same abundance pattern as those of IC 2391, with the exception of Ba. Keeping a margin of ±0.1 dex we find that 10 stars out of the 102 in the Bensby et al. (2005) sample could be classed as sharing the same abundance patterns (except Ba). If we include Ba abundances in the chemical tagging process, then only one star in the Bensby et al. (2005) sample share a common chemistry as IC 2391. Should we adopt a more strict criteria with an abundance margin of ±0.05 dex, which is the level of homogeneity seen within bound clusters, then none of the Bensby et al. (2005) stars share the open cluster abundance pattern, even without considering Ba. Clearly, abundance matching of this form is plagued by systematic effects between different studies. We await the availability of data from large surveys such as the GALAH survey [4] planned with the HERMES instrument (Barden et al. 2010; Heijmans et al. 2012), which would be homogeneously observed and analysed, to further expand this field of research.

4.2 Ba abundances

The abundance of Ba, the only analysed *s*-process element in our study, is clearly overabundant with respect to the field as noted in the discussion above. Similar enhancement in Ba is seen in other young clusters, including the Hyades cluster and supercluster (De Silva et al. 2006, 2011). D'Orazi et al. (2009) detected, in a sample of 20 open clusters, an anticorrelation between the [Ba/Fe] ratios and the cluster age. While OCs with ages $\gtrsim$4 Gyr are characterized by solar Ba abundances, the OCs with ages ∼100–200 Myr exhibit an enhancement up to 0.2–0.3 dex. This increasing trend can be reproduced only if the contribution from low-mass AGBs ($1.0 < M/M_{\odot} < 1.5$) to the Galactic chemical enrichment is higher than what was previously thought (see D'Orazi et al. 2009; Maiorca et al. 2011 for further details). Most intriguingly, the younger clusters of their sample ($\lesssim$70 Myr) show an even higher Ba content ([Ba/Fe] up to 0.5–0.6 dex), which cannot be explained by this scenario. It is quite unlikely that an enrichment in the Ba content took place in the last ∼100 Myr of Galactic evolution, unless mechanisms of local enrichment are invoked. Similarly, Desidera et al. (2011), analysing the star HD 61005 and its possible link to the Argus association, confirm the same abundance pattern, i.e. the [Ba/Fe] is more than a factor of 4 above the solar value. In Fig. 6, we report the run of [Ba/Fe] with age for clusters presented in D'Orazi et al. (2009),[5] for the three young moving groups by D'Orazi et al. (2012), along with

[4] www.aao.gov.au/HERMES/GALAH

[5] Due to a systematic offset between dwarfs and giants in the D'Orazi et al. (2009) sample, here we consider, for homogeneity, only clusters whose abundances come from unevolved members.

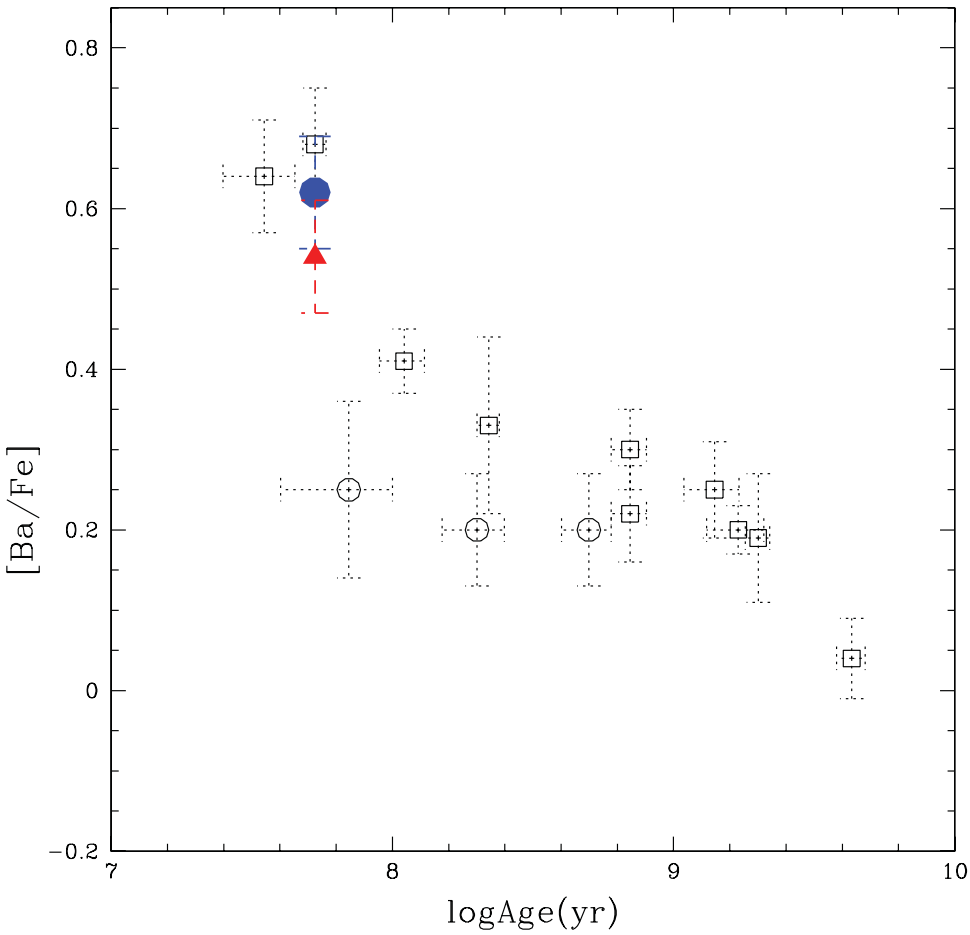

Figure 6. [Ba/Fe] as a function of cluster age for IC 2391 (filled circle) and the Argus association (filled triangle) as well as open clusters (labelled as open squares from D'Orazi et al. 2009) and moving groups (labelled as open circles from D'Orazi et al. 2012).

our measurements for IC 2391 and Argus field stars (this study). As one can see, our values fit the Ba–age relationship very well, confirming that very young open clusters seem to share an extremely high Ba abundance.

Moreover, the peculiar nature of Ba stands out from the other *s*-process elements: when available, abundances of Y, Zr (first-peak *s*-process element), and La, Ce (second-peak *s*-process element) show solar ratios [see De Silva et al. (2006); Carrera & Pancino (2011) for the Hyades; D'Orazi et al. (2012) for three moving groups AB Doradus, Carina-Near and Ursa Major]. Since none of the currently available models can reproduce such a trend (accounting for an overproduction of Ba without a similar trend in La and/or Ce), we are probably dealing with several spurious, conspiring effects which mimic a supersolar Ba content. A wide discussion of this topic is out of the purpose of this paper (we refer the reader to D'Orazi et al. 2012), here we just recall that the presence of hot chromospheres in these young stars might play, directly or indirectly, a certain role in the strength of the Ba II line(s).

4.3 The dissolution of IC 2391

With all present evidence pointing to a common origin of IC 2391 and the Argus association stars, we now explore the likely dissolution mechanism of the original open cluster. Lamers & Gieles (2006) have shown that most of the energy necessary to dissolve a cluster comes from collisions with GMCs. Depending on the impact parameter and the energy involved in the collision, a halo of stars is left around a central spheric or more oblate core. Qualitatively speaking, this is what we see in Fig. 1 with the IC 2391 being the core and the Argus association stars as part of the halo (Gieles et al. 2006). The lack of symmetry around the cluster (blue triangles), however, is partially due to the fact that the IC 2391 is on the limit of the SACY survey (Torres et al. 2008) of 150 pc. The second half of the halo being beyond 150 pc.

For a small-N system like IC 2391 a halo of unbound stars can also be the result of ejections of stars from the cluster core due to two-body encounters. Even when the tidal field is weak, clusters lose stars because of close encounters of stars in the cluster. This process is important for clusters whose age exceeds the half-mass relaxation time $\tau_{\rm rh}$. Based on an estimated half-mass radius of about 1.5 pc (Dias et al. 2002), a mass of about 500 $M_\odot$ (Boudreault & Bailer-Jones 2009), we use the standard expression for the half-mass relaxation time-scale $\tau_{\rm rh}$ of Spitzer & Hart (1971) and find $\tau_{\rm rh} \simeq 70$ Myr. Here, we assumed the mean mass of the stars to be 0.5 $M_\odot$ (i.e. $N = 1000$) and we use $0.02N$ as the argument of the Coulomb logarithm. Although this value for $\tau_{\rm rh}$ is uncertain to within a factor of 2 or 3, the similarity between $\tau_{\rm rh}$ and the age of IC 2391 (about 30 ± 10 Myr) suggests that it is possible that IC 2391 is dynamically evolved and has ejected a fraction of its stars. These unbound stars we now observe as the Argus association around the cluster. It implies that the cluster was smaller and denser in the past (Hénon 1965; Gieles et al. 2010).

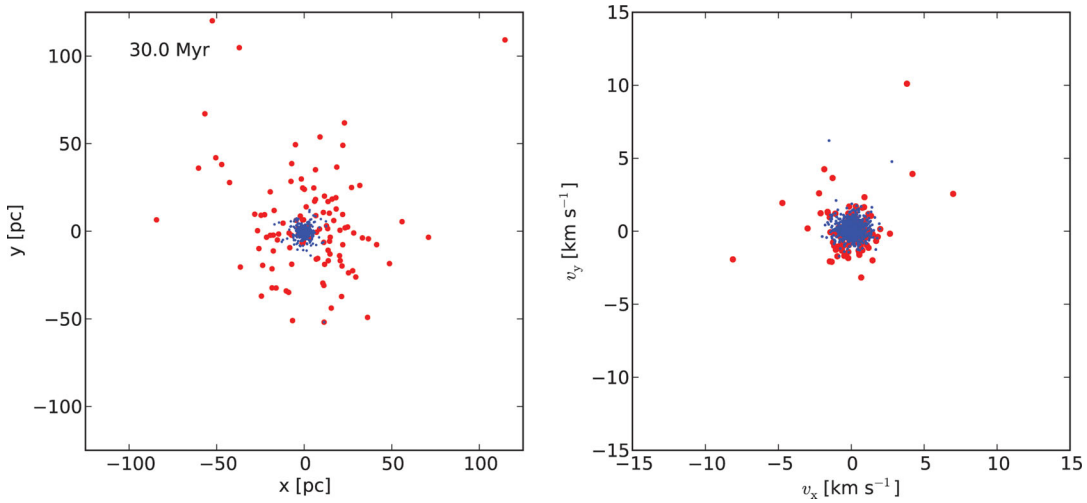

Figure 7. Results of an *N*-body simulation with NBODY6 (Aarseth 2003) of an isolated cluster with $N = 1024$, a Kroupa (2001) stellar mass function between 0.1 and 10 $M_\odot$. The initial density profile followed from a Plummer (1911) model with a half-mass radius of $r_h = 0.25$ pc. The small blue symbols represent all bound stars at an age of 30 Myr and the larger red circles are unbound members. The cluster and halo are comparable to IC 2391 and the Argus association at 30 Myr.

In fact, we can speculatively estimate the initial size and velocity dispersion of the cluster. The radius of the Argus associations is about 150 pc. Combined with an age of 30 Myr for IC 2391 this means that the most distant stars must have escaped with a velocity of about 5 km s^{-1}. The typical velocity with which stars escape from an isolated cluster is few v_{rms}, where v_{rms} is the rms velocity of cluster. So the most distant stars escaped when the cluster had $v_{rms} \simeq 1$–2 km s^{-1}. Combined with the mass this corresponds to a half-mass radius of about $r_h \simeq 0.2$–0.4 pc. In Fig. 7, we illustrate this idea with the result of an *N*-body simulation of an isolated cluster with an initial $r_h = 0.25$ pc. After 30 Myr there are unbound stars out to 100 pc away from the cluster, which have velocities of a several km s^{-1}. The current $r_h \simeq 1.1$ pc and 897 stars are still bound to the cluster, comparable to IC 2391.

This implies that the initial density of IC 2391 was several orders of magnitude higher than the present day density and the initial relaxation time a factor of a few shorter. This could be the explanation for the observed mass segregation in the cluster (Boudreault & Bailer-Jones 2009). These are of course very rough estimates, because we have ignored the presence of the Galactic tidal field and external factors such as GMCs.

5 SUMMARY AND CONCLUSIONS

In this paper, we presented the members of the Argus association as identified via the SACY survey and find the age of the system to be about 30 ± 10 Myr. Based on high-resolution UVES spectra, we determined the abundances for Fe, Na, Mg, Al, Si, Ca, Ti, Cr, Ni and Ba in both the open cluster IC 2391 and the Argus association. All stars in the open cluster and Argus association were found to share similar abundances with the scatter well within the uncertainties, where [Fe/H] $= -0.04 \pm 0.03$ for cluster stars and [Fe/H] $= -0.06 \pm 0.05$ for Argus stars. All other elements were in their solar proportions with the exception of Ba which we observed to be enhanced to around 0.6 dex. We also discussed the effects of overionization/excitation observed in our sample for stars cooler than about 5200 K, as has been previously noted in the literature.

In summary, we present strong kinematic, evolutionary and chemical evidence to support a common origin for the Argus association and the open cluster IC 2391. In particular, the chemical tagging of the stars presented in this paper provides *a necessary* condition to prove the link between the Argus association and IC 2391. However, as discussed in the text, many elemental abundances of the studied stars are indistinguishable from the solar neighbourhood, with the exception of Ba which is an important piece of evidence in favour of a common origin of the two stellar systems. For reasons which are not yet completely understood, barium abundances have been recently found to correlate with age. The abundances found for both stellar systems are similar. Moreover, they fit the Ba–age correlation very well.

Given all evidence in hand, we conclude that we are witnessing the on-going dissolution of IC 2391, where the stellar members of the Argus association stars were originally born in the same protocluster cloud as IC 2391. Simple modelling of this system finds the dissolution of this time-scale to be consistent with two-body interactions. A more detailed modelling of the disruption mechanisms, predicting spatial distribution and possibly the velocity dispersion of both groups would strengthen the proposed scenario. From an observational point of view, the second half of the stellar halo will be easily found by *GAIA* settling the question.

ACKNOWLEDGEMENTS

CM would like to thank the AAO Distinguished Visitor Program and the ESO DGDF for funding his visit to AAO/Australia. CT and CM are grateful to the ESO DGDF and Visitor Program for continuous support for to the SACY project in the form of DGDF, science-leaves and visitorships. MG thanks the Royal Society for financial support. We thank the anonymous referee for helpful suggestions and Simon O'Toole for proof reading the manuscript.

We also thank the Centre de Données Astronomiques de Strasbourg (CDS), the US Naval Observatory and NASA for the use of their electronic facilities, especially SIMBAD, UCAC4, the Washington Double Star Catalog (WDS) and ADS.

REFERENCES

Aarseth S. J., 2003, Gravitational N-Body Simulations. Cambridge Univ. Press, Cambridge

Allende Prieto C. et al., 2008, AJ, 136, 2070
Barden S. C. et al., 2010, in McLean I. S., Ramsay S. K., Takami H., eds, Proc. SPIE Vol. 7735, Society of Photo-Optical Instrumentation Engineers. SPIE, Bellingham, p. 773509
Bensby T., Feltzing S., Lundström I., Ilyin I., 2005, A&A, 433, 185
Bensby T., Oey M. S., Feltzing S., Gustafsson B., 2007, ApJ, 655, L89
Biazzo K., Randich S., Palla F., Briceño C., 2011, A&A, 530, A19
Boudreault S., Bailer-Jones C. A. L., 2009, ApJ, 706, 1484
Bubar E. J., King J. R., 2010, AJ, 140, 293
Carrera R., Pancino E., 2011, A&A, 535, A30
Castelli F., Gratton R. G., Kurucz R. L., 1997, A&A, 318, 841
Covino E., Alcala J. M., Allain S., Bouvier J., Terranegra L., Krautter J., 1997, A&A, 328, 187
D'Orazi V., Randich S., 2009, A&A, 501, 553
D'Orazi V., Magrini L., Randich S., Galli D., Busso M., Sestito P., 2009, ApJ, 693, L31
D'Orazi V., Biazzo K., Desidera S., Covino E., Andrievsky S. M., Gratton R. G., 2012, MNRAS, 423, 2789
da Silva L., Torres C. A. O., de La Reza R., Quast G. R., Melo C. H. F., Sterzik M. F., 2009, A&A, 508, 833
De Silva G. M., Sneden C., Paulson D. B., Asplund M., Bland-Hawthorn J., Bessell M. S., Freeman K. C., 2006, AJ, 131, 455
De Silva G. M., Freeman K. C., Bland-Hawthorn J., Asplund M., Bessell M. S., 2007a, AJ, 133, 694
De Silva G. M., Freeman K. C., Asplund M., Bland-Hawthorn J., Bessell M. S., Collet R., 2007b, AJ, 133, 1161
De Silva G. M., Freeman K. C., Bland-Hawthorn J., Asplund M., Williams M., Holmberg J., 2011, MNRAS, 415, 563
Desidera S. et al., 2011, A&A, 529, A54
Dias W. S., Alessi B. S., Moitinho A., Lépine J. R. D., 2002, A&A, 389, 871
Díaz C. G., González J. F., Levato H., Grosso M., 2011, A&A, 531, A143
Freeman K., Bland-Hawthorn J., 2002, ARA&A, 40, 487
Gieles M., Portegies Zwart S. F., Baumgardt H., Athanassoula E., Lamers H. J. G. L. M., Sipior M., Leenaarts J., 2006, MNRAS, 371, 793
Gieles M., Baumgardt H., Heggie D. C., Lamers H. J. G. L. M., 2010, MNRAS, 408, L16
Gieles M., Moeckel N., Clarke C. J., 2012, MNRAS, 426, L11
Guenther E. W., Esposito M., Mundt R., Covino E., Alcalá J. M., Cusano F., Stecklum B., 2007, A&A, 467, 1147
Heijmans J. et al., 2012, McLean I., Ramsay S., Takami H., eds, Proc. SPIE Vol. 8446, Society of Photo-Optical Instrumentation Engineers. SPIE, Bellingham, p. 84460W
Hénon M., 1965, Ann. Astrophys., 28, 62
Huélamo N. et al., 2010, A&A, 521, L54
James D. J., Melo C., Santos N. C., Bouvier J., 2006, A&A, 446, 971
Kiraga M., 2012, Acta Astron., 62, 67
Kroupa P., 2001, MNRAS, 322, 231
Lada C. J., Lada E. A., 2003, ARA&A, 41, 57
Lamers H. J. G. L. M., Gieles M., 2006, A&A, 455, L17
Maiorca E., Randich S., Busso M., Magrini L., Palmerini S., 2011, ApJ, 736, 120
Mamajek E. E., Lawson W. A., Feigelson E. D., 2000, ApJ, 544, 356
Mashonkina L. I., Vinogradova A. B., Ptitsyn D. A., Khokhlova V. S., Chernetsova T. A., 2007, Astron. Rep., 51, 903
McWilliam A., Preston G. W., Sneden C., Shectman S., 1995, AJ, 109, 2736
Moeckel N., Holland C., Clarke C. J., 2012, MNRAS, 425, 450
Neuhäuser R., 1997, Sci, 276, 1363
Oort J. H., 1958, Ric. Astron., 5, 507
Pancino E., Carrera R., Rossetti E., Gallart C., 2010, A&A, 511, A56
Patten B. M., Simon T., 1996, ApJS, 106, 489
Platais I., Melo C., Mermilliod J.-C., Kozhurina-Platais V., Fulbright J. P., Méndez R. A., Altmann M., Sperauskas J., 2007, A&A, 461, 509 (P07)
Plummer H. C., 1911, MNRAS, 71, 460
Pompéia L. et al., 2011, MNRAS, 415, 1138
Randich S., Pallavicini R., Meola G., Stauffer J. R., Balachandran S. C., 2001, A&A, 372, 862
Riedel A. R., Murphy S. J., Henry T. J., Melis C., Jao W.-C., Subasavage J. P., 2011, AJ, 142, 104
Schuler S. C., King J. R., Fischer D. A., Soderblom D. R., Jones B. F., 2003, AJ, 125, 2085
Schuler S. C., King J. R., Hobbs L. M., Pinsonneault M. H., 2004, ApJ, 602, L117
Schuler S. C., Plunkett A. L., King J. R., Pinsonneault M. H., 2010, PASP, 122, 766
Shen Z.-X., Jones B., Lin D. N. C., Liu X.-W., Li S.-L., 2005, ApJ, 635, 608
Siess L., Dufour E., Forestini M., 2000, A&A, 358, 593
Sneden C. A., 1973, PhD thesis, Univ. Texas Austin
Sousa S. G., Santos N. C., Israelian G., Mayor M., Monteiro M. J. P. F. G., 2007, A&A, 469, 783
Spitzer L. Jr, 1958, ApJ, 127, 17
Spitzer L. J., Hart M. H., 1971, ApJ, 164, 399
Steenbock W., Holweger H., 1981, A&A, 99, 192
Torres C. A. O., Quast G., de La Reza R., da Silva L., Melo C. H. F., Sterzik M., 2003, in Lépine J., Gregorio-Hetem J., eds, Vol. 299, Proc. Open Issues in Local Star Formation, Kluwer, Dordrecht, p. 83
Torres C. A. O., Quast G. R., da Silva L., de La Reza R., Melo C. H. F., Sterzik M., 2006, A&A, 460, 695
Torres C. A. O., Quast G. R., Melo C. H. F., Sterzik M. F., 2008, in Reipurth B., ed., Young Nearby Loose Associations, p. 757
van Leeuwen F., 2007, A&A, 474, 653
Viana Almeida P., Santos N. C., Melo C., Ammler-von Eiff M., Torres C. A. O., Quast G. R., Gameiro J. F., Sterzik M., 2009, A&A, 501, 965
Zacharias N., Finch C. T., Girard T. M., Henden A., Bartlett J. L., Monet D. G., Zacharias M. I., 2012, VizieR Online Data Catalog, 1322, 0
Zuckerman B., Rhee J. H., Song I., Bessell M. S., 2011, ApJ, 732, 61

APPENDIX A: ATOMIC LINE LIST

Table A1. Atomic line list. Full table data available online.

Element	Wavelength (Å)	LEP (eV)	log *g f*	EW PMM 3359 (mÅ)
Na I	5682.63	2.1	−0.71	123.2
Na I	5688.21	2.1	−0.40	144.7
Na I	6154.23	2.1	−1.57	56.0
Mg I	5711.09	4.35	−1.71	126.5
–	–	–	–	–
–	–	–	–	–
–	–	–	–	–

SUPPORTING INFORMATION

Additional Supporting Information may be found in the online version of this article:

Table A1. Atomic line list. Full table data available online (http://mnras.oxfordjournals.org/lookup/suppl/doi:10.1093/mnras/stt153/-/DC1).

Please note: Oxford University Press is not responsible for the content or functionality of any supporting materials supplied by the authors. Any queries (other than missing material) should be directed to the corresponding author for the article.

This paper has been typeset from a TEX/LATEX file prepared by the author.